

Dielectric anomalies in [111] oriented $0.955\text{Pb}(\text{Zn}_{1/3}\text{Nb}_{2/3})\text{O}_3 - 0.045\text{PbTiO}_3$ single crystals under different electrical and thermal conditions

Mingrong Shen^{a)}

Department of Physics, Suzhou University, Suzhou 215006, People's Republic of China

Wenwu Cao^{b)}

Department of Physics and Materials Science, City University of Hong Kong, 83 Tat Chee Avenue, Kowloon Tong, Hong Kong, China

(Received 20 August 2003; accepted 9 March 2004)

A detailed investigation has been conducted on the dielectric anomalies induced by different electrical and thermal conditions in [111] oriented $0.955\text{Pb}(\text{Zn}_{1/3}\text{Nb}_{2/3})\text{O}_3 - 0.045\text{PbTiO}_3$ (PZN-4.5%PT) single crystals. Application of a dc electrical field to the crystal results in field induced dielectric anomalies to occur at specific temperatures, which can be explained by the structural phase transitions from rhombohedral to orthorhombic, from orthorhombic to tetragonal, and from tetragonal to cubic phase, respectively. All transition temperatures are independent of frequency and have a threshold field that is dependent on the thermal history. The electric field–temperature diagrams based on dielectric anomalies were developed under different schemes of temperature and field variations. © 2004 American Institute of Physics.

[DOI: 10.1063/1.1728315]

I. INTRODUCTION

Relaxor ferroelectrics were first synthesized in the late 1950s and have attracted a lot of attention due to their unusual behavior of dielectric permittivity.^{1,2} In contrast to typical ferroelectric (FE) crystals, such as PbTiO_3 (PT), relaxor ferroelectrics exhibit a broad and frequency-dependent phase transition. Lead zinc niobate, $\text{Pb}(\text{Zn}_{1/3}\text{Nb}_{2/3})\text{O}_3$ (PZN), is an example of relaxor ferroelectric material. In PZN crystals, the difference in valence ($5+$ vs $2+$) and ionic radii (0.64 vs 0.74 Å) between the Nb^{5+} and Zn^{2+} ions on the B site of the ABO_3 perovskite structure results in symmetry breaking compositional and/or structural disorder, forming local polar clusters, or nanodomains. These local clusters can serve as nuclei for the ferroelectric phase and will coarsen with decreasing temperature starting from temperatures much higher than the dielectric maximum (T_{max}). These clusters, resulting from short-range correlated ionic displacements, are dispersed as islands in the host lattice and produce the unusual relaxor behavior of PZN crystals.^{3–6} Normal ferroelectric state could not be developed in PZN crystals without the application of external field,⁷ which is generally characterized by the disappearance of frequency dispersion.^{3,8}

Single crystal of $\text{Pb}(\text{Zn}_{1/3}\text{Nb}_{2/3})\text{O}_3 - \text{PbTiO}_3$ (PZN-PT) showed excellent dielectric and piezoelectric properties in domain engineered state, which have great potential for pushing new advances in transducer/actuator technology.^{9,10} Relaxor PZN can form a complete solid solution with the normal ferroelectric PT. There is a morphotropic phase

boundary (MPB) between the tetragonal and rhombohedral phases near 8% PT composition at room temperature. For composition $>9\%$ PT, the solid solution system behaves as normal ferroelectrics at room temperature, while some degree of relaxor behavior persists if the PT content is $<8\%$. In order to find out the nature of the relaxor phase transition and the influence of the internal charge carriers and electrical field in both the paraelectric and ferroelectric phases, it is important to systematically study the dielectric properties of PZN-PT under various electric field and thermal conditions.^{11,12} A lot of work have been carried out to study the electric field induced phase transitions in PZN-PT crystals along [001] of the cubic coordinates to make superpiezoelectric materials.¹³ This work will focus on the electric field induced dielectric anomalies in [111] oriented relaxor PZN-PT crystals.

In our recent work,¹⁴ moderate dc electrical field (0.65 kV/cm) induced dielectric anomalies were observed in [111] oriented $0.955\text{PZN}-0.045\text{PT}$ (PZN-4.5%PT) single crystals. Three distinct phases were revealed, which were distinguished by their frequency dispersion behavior and the dielectric anomalies. In this paper, we have extended the work to different levels of applied electric field applied to the crystals under different thermal histories. The focus of this paper is to develop electric field–temperature diagrams that describe the electric field induced dielectric anomalies in [111] oriented PZN-4.5%PT crystals. This composition of PZN-4.5%PT was chosen because it is away from the MPB and has relatively strong relaxor nature.

II. EXPERIMENTAL DETAILS

The [111] oriented PZN-4.5%PT sample crystals used in our experiments were grown using the high temperature flux method. The crystals were cut into a plate shape with the

^{a)} Author to whom correspondence should be addressed; electronic mail: mrshen@suda.edu.cn

^{b)} Permanent address: Department of Mathematics, The Pennsylvania State University, University Park, PA 16802.

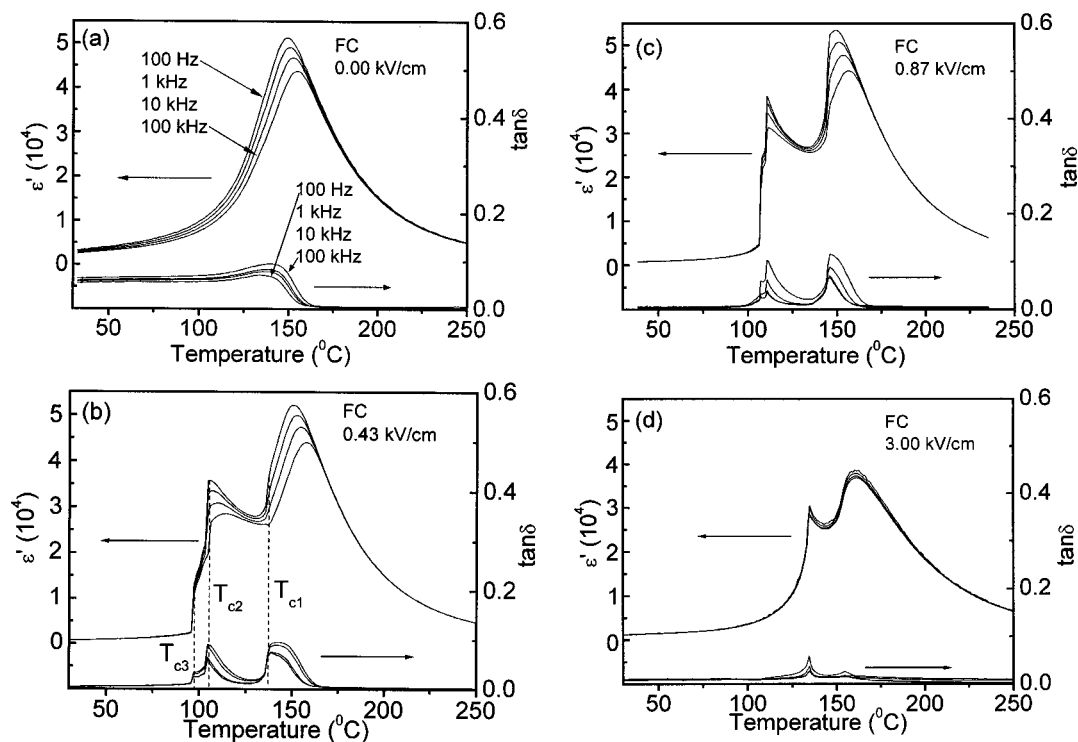


FIG. 1. Dielectric constant and loss as a function of temperature for the FC scheme under various dc biases.

orientations of $[111]$, $[\bar{1}\bar{1}0]$, and $[\bar{1}\bar{1}2]$, respectively. Their dimensions are 0.7–0.9 mm in thickness and 3–4 mm on each side dimension in the $[111]$ face. The $[111]$ and $[\bar{1}\bar{1}\bar{1}]$ faces were polished and electroded with gold. The dielectric response was measured as a function of temperature, frequency, and different dc electrical bias fields. Computer assisted dielectric measurements using a HP 4284 *LCR* meter were made in the temperature range of 30–250 °C on heating and cooling at a rate of 2 °C/min using a Delta 9023 oven. The temperature was measured using a platinum resistance thermocouple and a Keithley 740 system scanning thermometer. The thermocouple was mounted inside an aluminum plate, which supports the sample. In order to protect the *LCR* meter, a blocking circuit (HP16065A) was used when a high dc bias field was applied.

III. RESULTS AND DISCUSSIONS

In the experimental investigation of field and thermal history effects on relaxor PZN-4.5%PT, we have used three different schemes: (1) field cooling (FC), (2) zero-field heating after FC (ZFH-FC), and (3) field heating after zero-field cooling (FH-ZFC).

A. FC measurement

Figures 1(a)–1(d) show, respectively, the dielectric constant and loss as a function of temperature for the FC scheme under dc biases of 0, 0.43, 0.87, and 3.00 kV/cm. When the sample is cooled without the application of electrical field, the $[111]$ oriented PZN-4.5%PT crystal showed typical relaxor-type ferroelectric phase transition at T_{\max} (near 150 °C), as shown in Fig. 1(a). The results are consistent with those reported for relaxor PZN-PT crystals.¹⁵ The rhom-

bohedral phase below T_{\max} shows significant frequency dispersion, indicating that it is a relaxor phase. Upon the application of a small electrical field of 0.43 kV/cm during FC, one can see from Fig. 1(b) that three critical temperatures occur in the dielectric loss versus temperature curves below T_{\max} . The highest loss peak occurs at $T_{c1} \sim 137$ °C, which is superimposed on the broad background of the dielectric maximum. This peak moves to a higher temperature of 146 °C as the dc bias increases to 0.87 kV/cm, as shown in Fig. 1(c). Below T_{c1} , the degree of dielectric frequency dispersion decreases abruptly. Another dielectric anomaly appears at T_{c2} (near 104 °C) for the 0.43 kV/cm dc bias, which moves to a higher temperature near 110 °C as the dc bias increases to 0.87 kV/cm. The lowest critical temperature T_{c3} indicates a different type of transition, below which the frequency dispersion of the dielectric properties totally disappears.

In our previous work,¹⁴ we proposed the existence of a medium-range ordered phase between the long-range ordered and short-range ordered phases to explain the above dielectric anomalies. However, these phases have not actually been observed up to date. Therefore, in the present study, we discuss the dielectric anomalies in the context of observed and confirmed structural phase transitions. According to some reported optical¹⁶ and x-ray measurements¹⁷ on ZFH of $[111]$ poled PZN-PT crystals, ferroelectric rhombohedral (FE_r), orthorhombic (FE_o), and tetragonal (FE_t) structural phases have been found below T_{\max} . Using these transition anomalies, our results may be explained as follows: without the bias field, the PZN-4.5%PT crystals will transform directly from cubic to rhombohedral phase at T_{\max} , as illustrated in Fig. 1(a). When a bias field is applied along $[111]$, the FE_r

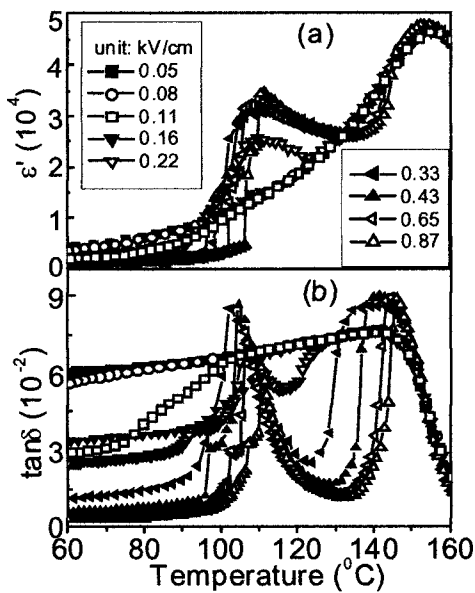


FIG. 2. Dielectric constant (a) and loss (b) vs temperature for the FC scheme under various dc biases at a frequency of 10 kHz.

phase seems to be stabilized by the field projection in $\langle 001 \rangle$ at the temperature below T_{c1} . Thus, the dielectric anomaly at T_{c1} is due to the structural phase transition from cubic to FE_t . As the temperature decreases, the field along $[111]$ will pull the system into another ferroelectric phase (FE_o) at T_{c2} , and eventually into FE_r at T_{c3} . Phase transitions from FE_r to FE_o and from FE_o to FE_t symmetry will be induced at temperatures near 108°C and 113°C , respectively, during ZFH. These transitions are confirmed by the optic method¹⁶ and high-resolution x-ray diffraction experiment.¹⁷ We note that the dielectric frequency dispersion is different in the three induced structural phases, as shown in Figs. 1(b) and 1(c), indicating different degrees of ordering. From Fig. 1, it can also be noted that the induced transition at T_{c1} and T_{c2} became sharper with increasing dc bias and T_{c3} moves closer to T_{c2} when the dc bias increases. Since the $[111]$ oriented field helps to stabilize the ferroelectric rhombohedral phase, the tetragonal region shrinks with the increase of the $[111]$ oriented bias field. At the same time, the transition to FE_r phase becomes easier. Eventually, T_{c3} moves up beyond T_{c2} as shown in Fig. 1(d) and the relaxor nature nearly vanished.

The above three induced phase transitions had threshold field (E_{th}). This is illustrated in Fig. 2, which shows the dielectric constant and loss as a function of temperature under various dc bias levels (E_{dc}) at a frequency of 10 kHz. For $E_{dc} < 0.08$ kV/cm, the dielectric properties can be found nearly independent of E_{dc} . However, when the bias level is between 0.08 and 0.11 kV/cm, anomalies appeared on both the dielectric constant and loss curves. From Fig. 2 one can see the presence of a threshold field E_{th} of about 0.11 kV/cm for T_{c1} , T_{c2} , and T_{c3} . This is demonstrated more clearly in Fig. 3. One can see that T_{c1} increases rapidly with increasing E_{dc} and eventually becomes saturated close to T_{max} when E_{dc} is above 1.3 kV/cm. T_{c2} also increases with increasing E_{dc} . However, the change of T_{c2} is much slower and has a trend to approach T_{max} under higher applied electric field. T_{c3}

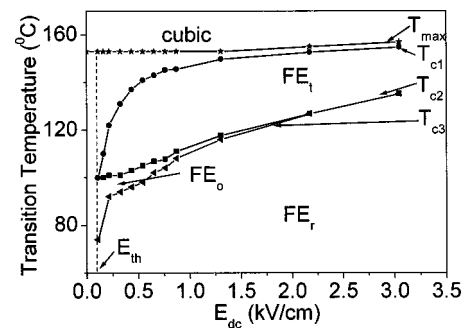


FIG. 3. Dependence of critical temperatures T_{c1} , T_{c2} , and T_{c3} on dc bias for the FC scheme.

moves closer to T_{c2} and finally overlapped by T_{c2} as E_{dc} increases. From Fig. 3 one can derive the electric field–temperature diagram for the induced dielectric anomalies during FC in PZN-4.5%PT crystals. It is evident that three structural states will occur in sequence if we cool the sample at temperatures above T_{max} and under electric fields above the threshold value of 0.11 kV/cm, i.e., from cubic to FE_t to FE_o to FE_r symmetry phases. The changes between different order states are not continuous, but rather drastic, resulting in the appearance of dielectric anomalies at T_{c1} , T_{c2} , and T_{c3} .

B. ZFH-FC measurements

In relaxors the induced normal ferroelectric state in the FC case remains stable at low temperature even after the removal of the bias electric field. A subsequent heating of the sample without the electric field (ZFH-FC) does not destroy this state until a critical temperature T_{c3} . According to the above FC results, T_{c2} and T_{c1} should also appear at higher temperatures. This is illustrated in Fig. 4, where ZFH-FC dielectric data are collected for different electric field during FC. We found that both T_{c1} and T_{c2} are indeed present as shown in Figs. 4(b)–4(d). The dielectric curves for three different levels of bias electric field in FC were almost the same, and T_{c1} , T_{c2} , and T_{c3} were all found to be independent of bias field. In order to explore whether there is a threshold voltage for the above three induced transitions, we measured the dielectric constant and loss as a function of temperature under various dc biases in FC scheme. The results are shown in Fig. 5. It is found that a threshold voltage of 0.07 kV/cm is clearly present. However, if the electrical field is less than 0.22 kV/cm, T_{c2} is found to be dependent on E_{dc} . It decreases gradually from 115°C to 113°C as the E_{dc} increases from 0.07 kV/cm to 0.22 kV/cm. There exists weak frequency dispersion even below T_{c2} when E_{dc} is less than 0.22 kV/cm. This is due to that fact that the FE_r phase is not fully formed at low temperatures during FC when E_{dc} is below 0.22 kV/cm. From Fig. 5 we can see that T_{c1} is almost independent of E_{dc} for all field levels.

Figure 6 shows the diagram for the bias field induced phase transitions during ZFH-FC. This diagram indicates that if the field strength is strong enough to induce the FE_r phase in the FC process, three subsequent phase transitions will occur during ZFH, i.e., from FE_r to FE_o , then from FE_o to FE_t , and finally from FE_t to cubic state. The critical tempera-

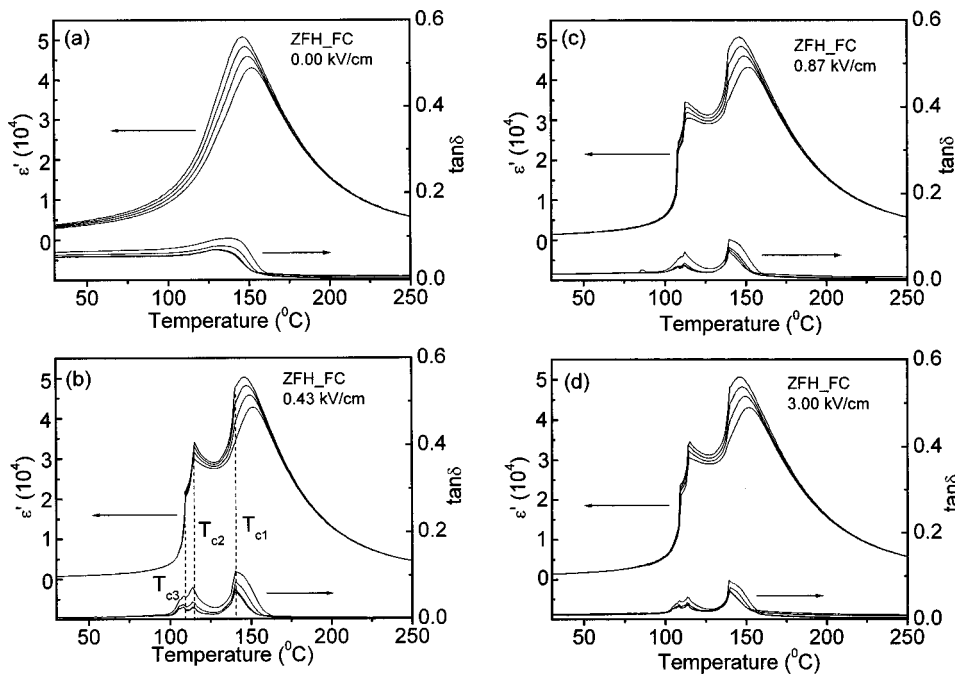


FIG. 4. Dielectric constant and loss as a function of temperature for the ZFH-FC scheme under various dc biases during FC.

tures of the phase transitions, T_{c3} , T_{c2} , and T_{c1} , are almost independent of the magnitude of the dc biases during FC, so long as it is above the threshold value.

C. FH-ZFC measurements

When the crystal is cooled without an external electrical field from a temperature above T_{max} , polar clusters are formed and persist down to room temperature, which is characterized by the frequency dispersion of the dielectric properties as shown in Fig. 4(a). Upon heating the sample under a dc bias field along [111], the tendency to form FE_r increases so that the frequency dispersion will be reduced. This characteristic is shown in Fig. 7. When the applied electric field is 0.43 kV/cm, frequency dispersion does not change much in the low temperature region until the temperature

reaches a critical value of 120 °C. However, when the applied electric field is increased to 0.65 kV/cm, frequency dispersion is visible at the beginning, as shown in Fig. 7(b), then a small but clear jump in the dielectric constant appeared at T_{c4} near 88 °C, above which the dielectric dispersion disappears. This is an indication of the formation of the FE_r phase. With further increase of temperature under the same dc bias field, the FE_r phase is broken down again at T_{c3} to FE_o , and then from FE_o to FE_t at T_{c2} , and from FE_t to cubic at T_{c1} . Figure 7(c) shows similar characteristics with Fig. 7(b), where 0.87 kV/cm bias electric field is applied during FH, but T_{c4} moves to a lower temperature. Figure 7(d) shows the dielectric properties with high dc voltage of 3.00 kV/cm applied on the sample during FH. Under such a high electric field, the crystal is in the FE_r phase even at room temperature and the critical nature of the induced transitions (at T_{c1} , T_{c2} , and T_{c3}) and the normal phase transition at T_{max} are all suppressed, which is consistent with what is observed in the FC process.

Similar to the characteristics of phase transitions at T_{c1} , T_{c2} , and T_{c3} in the cases of FC and ZFH-FC, the phase

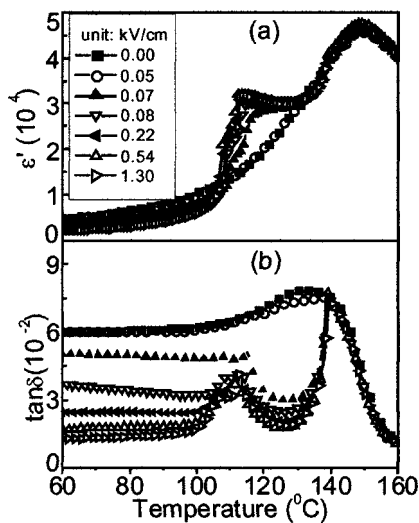


FIG. 5. Dielectric constant (a) and loss (b) vs temperature for the ZFH-FC scheme under various dc biases during FC at a frequency of 10 kHz.

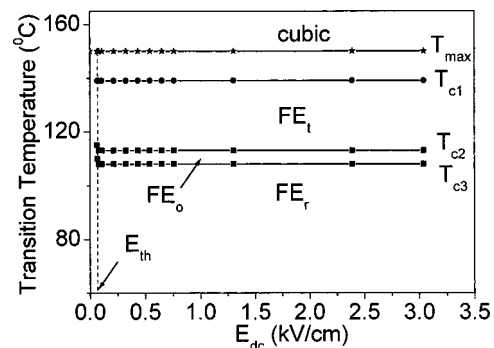


FIG. 6. Dependence of critical temperatures T_{c1} , T_{c2} , and T_{c3} on dc bias during FC for the ZFH-FC scheme.

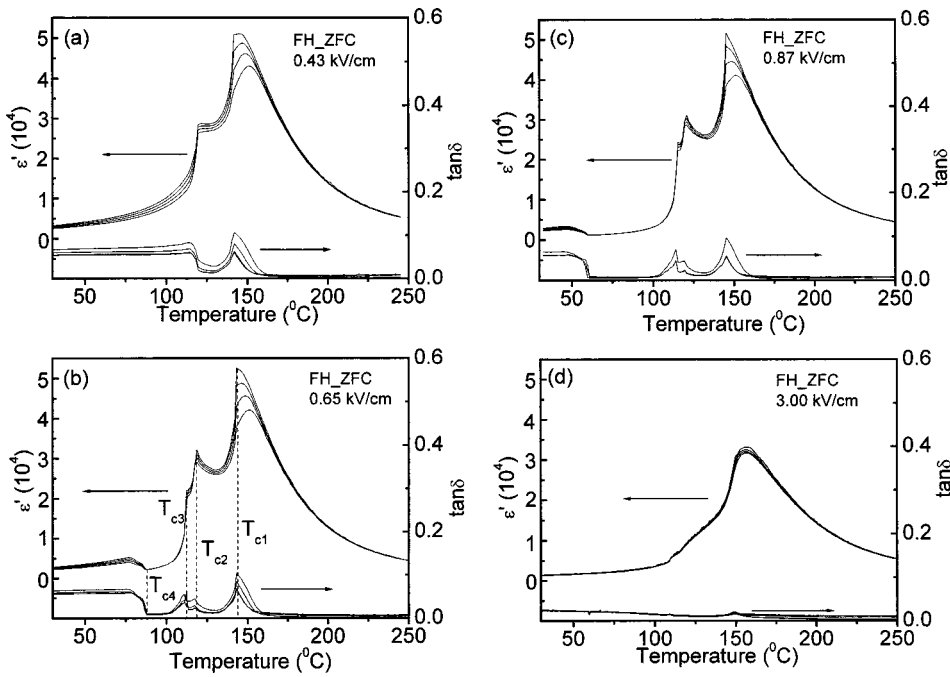


FIG. 7. Dielectric constant and loss as a function of temperature for the FH-ZFC scheme under various dc biases.

transitions at T_{c1} , T_{c2} , T_{c3} , and T_{c4} in the FH measurement also show threshold fields. This is illustrated in Fig. 8. For $E_{dc} < 0.22$ kV/cm, the dielectric properties are nearly independent of E_{dc} . We notice that this value of threshold voltage (0.22 kV/cm) is much higher than that in the FC case. From Figs. 8(a) and 8(b), one can see only two dielectric anomalies when the electric field is between 0.22 and 0.43 kV/cm. In this relatively weaker bias electric field region, the field is not strong enough to induce a FE_r phase in the sample, but may induce the FE_o first. We propose that the two dielectric anomalies in the electric region of 0.22–0.43 kV/cm are due to the phase transitions from FE_o to FE_t state (T_{c2}), and then to cubic phase at the higher temperature of T_{c1} . When the applied electric field is higher than 0.54 kV/cm, four anomalies appear as shown in Fig. 8; they correspond to the phase transitions from relaxor rhombohedral

phase to FE_r at T_{c4} , FE_r to FE_o at T_{c3} , FE_o to FE_t at T_{c2} , and FE_t to cubic phase at T_{c1} , respectively. It is evident that the threshold voltages for the appearance of FE_o and FE_r are 0.22 (E_{th1}) and 0.54 kV/cm (E_{th2}), respectively, as shown in Figs. 8 and 9.

Figure 9 shows the electric field–temperature diagram for the induced dielectric anomalies during FH. Under a relatively strong electric field, FE_r can be induced at a particular temperature T_{c4} , so that the system shows typical ferroelectric phase behavior beyond T_{c4} . In other words, the polar cluster state has been transformed into a normal ferroelectric phase induced by the external field at T_{c4} . Since the disorder increases with temperature, at a higher temperature T_{c3} , the FE_r phase will overcome the bias field to become a FE_o phase, and then to a FE_t phase, followed by the increase of dielectric dispersion, the characteristic of decreasing order.

From Figs. 1, 4, and 7, we can find some common characteristics for the T_{c1} , T_{c2} , and T_{c3} in the temperature dependence of dielectric properties measured under FC, ZFH-FC and FH-ZFC schemes, and T_{c4} for FH-ZFC scheme.

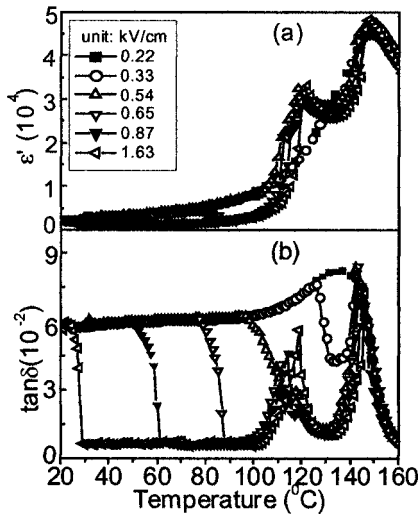


FIG. 8. Dielectric constant (a) and loss (b) vs temperature for the FH-ZFC scheme under the various dc biases at a frequency of 10 kHz.

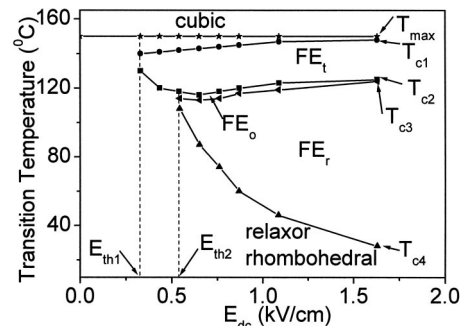


FIG. 9. Dependence of the critical temperatures T_{c1} , T_{c2} , T_{c3} , and T_{c4} on dc biases for the FH-ZFC scheme.

- (1) Unlike T_{\max} , these critical temperatures do not depend on frequency.
- (2) All induced transitions had first-order-like characteristics under low bias electrical field. Thermal hysteresis is present between cooling and heating in the vicinity of the dielectric discontinuities, indicating the system is metastable in temperature regions of over heating and under cooling. Metastability can only occur in a first-order transition but not in a second-order transition.¹⁸
- (3) The transitions at these temperatures are irreversible in the absence of an external electric field.

It is found that for the PMN-PT crystals,¹⁹ normal ferroelectric state can be induced either by increasing PT content cross the MPB so that the ferroelectric nature of the PT becomes dominant, namely, composition induced transition, or by applying a dc bias in [111] through field induced transition. The effect of the bias is to add more strength to the ferroelectric feature in the solid solution system. Our results revealed an interesting competing characteristic between the relaxor PZN and the normal ferroelectric PT constituents in the PZN-PT solid solution. Such competition produced four distinct structural phases (relaxor rhombohedral, FE_r , FE_o , and FE_t) below T_{\max} and the transitions between these states can be regulated by external bias and temperature, causing the appearance of four additional critical temperatures T_{c1} , T_{c2} , T_{c3} , and T_{c4} .

IV. SUMMARY AND CONCLUSIONS

In this paper, we report a detailed investigation on the dielectric anomalies in [111] oriented PZN-4.5%PT single crystals induced by different levels of bias electrical field during temperature variations. The electric field-temperature diagrams of the anomalies were developed under three different schemes of changing the temperature and bias field, i.e., FC, ZFH-FC, and FH-ZFC. It is demonstrated that the application of a dc electrical field to [111] oriented PZN-4.5%PT single crystals induced dielectric anomalies to occur at specific temperatures, which can be explained by the tran-

sitions between five different phases: relaxor rhombohedral, FE_r , FE_o , FE_t , and cubic phase. The amplitudes of the dielectric anomalies are frequency dependent, but the critical temperatures are practically independent of the field strength. There is a threshold field for the appearance of each of the dielectric anomalies, which depend on thermal histories.

ACKNOWLEDGMENTS

This research was supported by the Hong Kong RGC under Grant No. CityU 1056/02P and the Natural Science Foundation of China under Grant No. 10204016.

- ¹V. A. Bokov and I. E. Myl'nikova, *Sov. Phys. Solid State* **2**, 2428 (1961).
- ²G. A. Smolensky, *Sov. Phys. Solid State* **2**, 2584 (1961).
- ³G. A. Samara, E. L. Venturini, and V. H. Schmidt, *Appl. Phys. Lett.* **76**, 1327 (2000).
- ⁴N. de Mathan, E. Husson, G. Calvarin, J. R. Gavarrin, A. W. Hewat, and A. Morell, *J. Phys.: Condens. Matter* **3**, 8159 (1991).
- ⁵C. A. Randall, D. Barber, and R. Whatmore, *J. Microsc.* **45**, 275 (1987).
- ⁶C. A. Randall, A. Bhalla, T. R. Shrout, and L. E. Cross, *J. Mater. Res.* **29**, 5 (1990).
- ⁷S. F. Liu, S. E. Park, L. E. Cross, and T. R. Shrout, *J. Appl. Phys.* **92**, 461 (2002).
- ⁸E. V. Colla, N. K. Yushin, and D. Viehland, *J. Appl. Phys.* **83**, 3298 (1998).
- ⁹J. Kuwata, K. Uchino, and S. Nomura, *Jpn. J. Appl. Phys., Part 1* **21**, 12 989 (1982).
- ¹⁰S. E. Park and T. R. Shrout, *IEEE Trans. Ultrason. Ferroelectr. Freq. Control* **44**, 1140 (1997).
- ¹¹D. Viehland and Y.-H. Chen, *J. Appl. Phys.* **88**, 6696 (2000).
- ¹²D. Viehland, J. Powers, L. E. Cross, and J. F. Li, *Appl. Phys. Lett.* **78**, 3508 (2001).
- ¹³S. F. Liu, S. E. Park, T. R. Shrout, and L. E. Cross, *J. Appl. Phys.* **82**, 1804 (1997); B. Noheda, D. E. Cox, G. Shirane, S. E. Park, L. E. Cross, and Z. Zhong, *Phys. Rev. Lett.* **86**, 3891 (2001), and references therein.
- ¹⁴M. R. Shen, J. P. Han, and W. W. Cao, *Appl. Phys. Lett.* **83**, 731 (2003).
- ¹⁵M. L. Mulvihill, S. E. Park, G. Risch, Z. Li, K. Uchino, and T. R. Shrout, *Jpn. J. Appl. Phys., Part 1* **37**, 3984 (1996).
- ¹⁶Y. Lu, D. Y. Jeong, Z. Y. Cheng, T. Shrout, and Q. M. Zhang, *Appl. Phys. Lett.* **80**, 1918 (2003).
- ¹⁷J. S. Forrester, R. O. Piltz, E. H. Kisi, and G. J. McIntyre, *J. Phys.: Condens. Matter* **13**, L825 (2001).
- ¹⁸M. E. Lines and A. M. Glass, *Principles and Applications of Ferroelectrics and Related Materials* (Oxford, London, 1977).
- ¹⁹J. P. Han and W. Cao, *Phys. Rev. B* **68**, 134103 (2003).